

## Supporting Information

### Light Induced Quinone conformation of Polymer Donors toward 19.9% Efficiency Organic Solar Cells

Chuanhang Guo<sup>a</sup>, Yuandong Sun<sup>a</sup>, Liang Wang<sup>a</sup>, Chenhao Liu<sup>a</sup>, Chen Chen<sup>a</sup>, Jingchao Cheng<sup>b</sup>, Weiyi Xia<sup>a</sup>, Zirui Gan<sup>a</sup>, Jing Zhou<sup>a</sup>, Zhenghong Chen<sup>a</sup>, Jinpeng Zhou<sup>a</sup>, Dan Liu<sup>a</sup>, Jingxing Guo<sup>c</sup>, Wei Li<sup>a</sup> and Tao Wang<sup>a,b,\*</sup>

<sup>a</sup>School of Materials Science and Engineering, Wuhan University of Technology, Wuhan 430070, China E-mail: [twang@whut.edu.cn](mailto:twang@whut.edu.cn)

<sup>b</sup>School of Materials and Microelectronics, Wuhan University of Technology, Wuhan 430070, China

<sup>c</sup>School of Chemistry, Chemical Engineering & Life Sciences, Wuhan University of Technology, Wuhan 430070, China

### Solar Cell Fabrication and Characterization

#### Materials

PM6 ( $M_w = 97$  kDa, PDI = 2.4), D18 ( $M_w = 84$  kDa, PDI = 2.1), PBDB-T ( $M_w = 11.5$  kDa, PDI = 1.18), PTB7-Th ( $M_w = 30$  kDa, PDI = 1.6), L8-BO, 2PACz and PDINN were purchased from Solarmer Materials (Beijing) Inc. 3,5-Dichlorobromobenzene (DCBB) was purchased from Bide Pharmatech Co., Ltd. PEDOT:PSS (4083) was purchased from the Clevios<sup>TM</sup>. Unless otherwise stated, all chemicals and solvents were of reagent grade and used as received.

#### Procedure of UV-light treatment

8 mg/ml of PM6 (5 mg/ml for D18, 8 mg/ml for PBDB-T, 8 mg/ml for PTB7-Th) was introduced into a 2 ml glass vial (with transmittance over 90% for the incident UV-light) fitted with a magnetic stir bar. After the full dissolving of PM6, the vial was placed invertedly in glovebox with a UV lamp (5 mW cm<sup>-2</sup>, 365 nm) cast on. Then, the solution was gently stirred at 300 rpm and irradiated for 4 min. The treated polymer solutions were blended with L8-BO and used as the photoactive layer solution.

#### Device fabrication

All organic solar cells were fabricated in a conventional structure of ITO/glass/2PACz/active layer/PDINN/Ag. The pre-patterned indium tin oxide (ITO)-glass substrates (resistance  $\approx 15 \Omega$  per

square) were cleaned by sequential ultrasonic cleaning in water, ethanol, and isopropyl alcohol for 15 min each, and dried at 150 °C on a hotplate before use. These substrates were further treated with ultraviolet/Ozone for 30 min before solution processing. Then a monolayer 2PACz (0.5 mg ml<sup>-1</sup> in ethanol) was spin-coated at 3000 rpm onto ITO substrate, and dried on a heating plate at 80 °C for 6 min. After heating, the 2PACz coated substrates were washed dynamically by spin-coating 50 µL ethanol on its surface at 5000 rpm. The photoactive layer solution was prepared by dissolving the PM6:L8-BO, D18:L8-BO, PBDB-T:L8-BO, PTB7-Th:L8-BO, D18:PM6:L8-BO (13.4 mg/ml, 8.8 mg/ml, 9 mg/ml, 15.4 mg/ml, 15.4 mg/ml respectively, with the presence of DCBB that keeps a 1:1 weight ratio with L8-BO ) with the donor:acceptor weight ratios of 1:1.2 in chloroform, to receive films with thickness around 100 nm. Then PDINN (1.5 mg/mL) in MeOH solution was cast on the photoactive layer at a speed of 3000 rpm for 60 s to form the electron transport layer. Afterwards, the devices were transferred to the evaporation chamber and 100 nm Ag layer was thermally evaporated under high vacuum through the shadow mask to form the anode. The size of the photoactive area defined by the overlapping of anode and cathode is 6.625 mm<sup>2</sup>.

## Characterization

Film thickness and the *in-situ* ellipsometry measurement were measured using a spectroscopic ellipsometer (J. A. Woollam, USA). Photoluminance (PL) measurements were measured with a PL microscopic spectrometer (Flex One, Zolix, China) with a 532 nm CW laser. The Fourier transform infrared (FT-IR) spectra were measured with a Fourier infrared spectrometer (Nicolet, America). The Raman spectra were measured with a Confocal microscope Raman spectrometer (LabRAM Odyssey, Japan). The surface morphology of the active layers was characterized by atomic force microscopy (AFM) (NT-MDT, Russia) and transmission electron microscopy (TEM) (JEOL, Japan). Grazing-incidence wide-angle X-ray scattering (GIWAXS) and Grazing-incidence small-angle X-ray scattering (GISAXS) were conducted using the beamline BL16B1 at the Shanghai Synchrotron Radiation Facility in China. Absorption spectra were measured using a UV-visible spectrophotometer (HITACHI, Japan). *J-V* characterization of the device was performed under AM 1.5G (100 mW cm<sup>-2</sup>) using a Newport 3A solar simulator (USA) in air at room temperature with an aperture mask area of 4 mm<sup>2</sup>. The light intensity was calibrated using a standard silicon reference cell certified by the National Renewable Energy Laboratory (NREL, USA). *J-V* characteristics were recorded using *J-V* sweep software developed by Ossila Ltd. (UK) and a Keithley 2612B (USA) source meter unit. EQE was measured with a Zolix (China) EQE system equipped with a standard Si diode.

## GISAXS Modelling

The 1D profile of PM6 with or without UV-light treated were simulated through a universal method according to previous work,<sup>1</sup> in which the scattering intensity of PM6 films can be expressed

as Equation 1.

$$I(q) = P(q)S(q) + B \quad (1)$$

Where  $P(q)$  is related to the form factor of primary crystalline particles (approximated by spherical shape of radius  $R$ ), and  $S(q)$  is the fractal structure factor, describing the interaction between primary particles in the fractal-like aggregation system. The constant  $B$  is due to incoherent scattering background.  $P(q)$  includes the product of particle volume fraction  $\phi$ , the square of scattering length density difference between crystalline and amorphous polymers  $\Delta\rho^2$  and crystalline particle volume  $V_p$ .  $S(q)$  is given by Equation 2.

$$S(q) = 1 + \frac{\sin[(D-1)\tan^{-1}(q\xi)]}{(qR)^D} \frac{D\Gamma(D-1)}{[1 + 1/(q\xi)^2]^{(D-1)/2}} \quad (2)$$

Where  $\xi$  is the correlation length of the fractal-like network (or domain) formed by the aggregation of primary crystalline particles.  $D$  is the fractal dimension.  $R$  is the mean radius of primary crystalline particles. The domain size of this network or domain is approximately characterized by  $R_g$ , where  $R_g$  is the Guinier radius of this fractal-like network (see Equation 3).

$$R_g = \sqrt{\frac{D(D+1)}{2}}\eta \quad (3)$$

For the NFAs-based blend films, the simulation was conducted via a Debye-Anderson-Brumberger model+ Fractal model<sup>2</sup> using Equation 4, where  $q$  is the scattering wave vector,  $A_1$  is an independent fitting parameter,  $\xi$  is the average correlation length of the polymer domain,  $P(q, R)$  and  $S(q, R)$  are the form factor and fractal structure factor, respectively. The correlation length of the fractal-like structure is represented by  $\eta$  and  $D$  is the fractal dimension.

$$I(q) = \frac{A_1}{[1 + (q\xi)^2]^2} + A_2(P(q, R))S(q, R, \eta, D) + B \quad (4)$$

## Supporting Figures and Tables

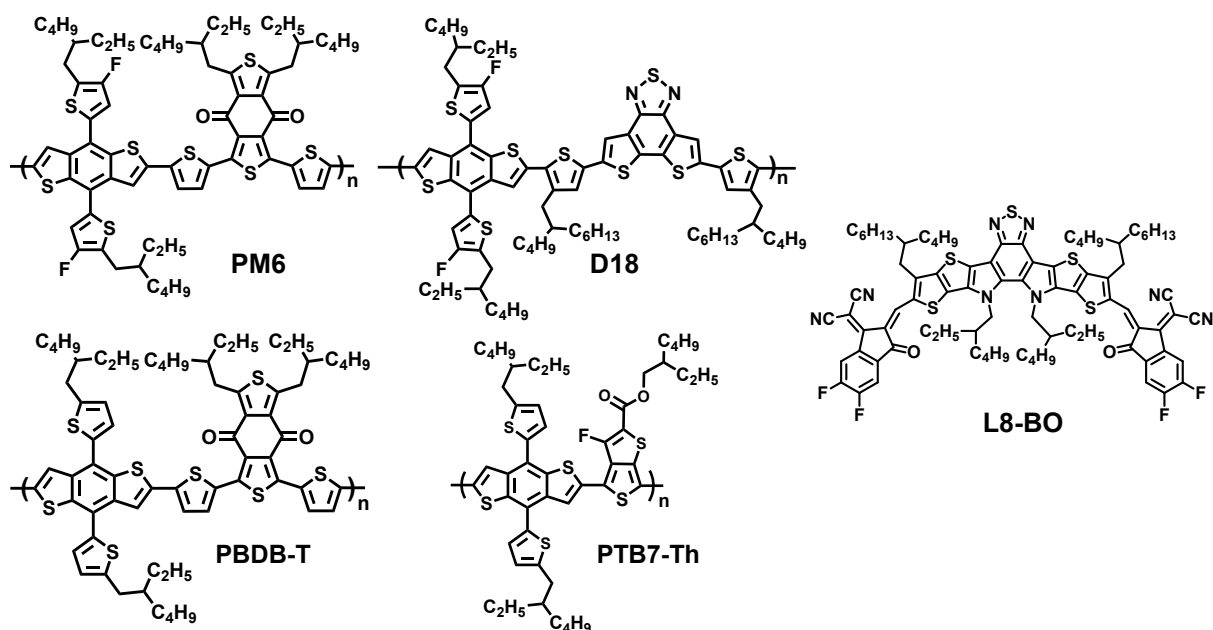


**Figure S1.** Chemical structures of PM6, D18, PBDB-T, PTB7-Th and L8-BO.

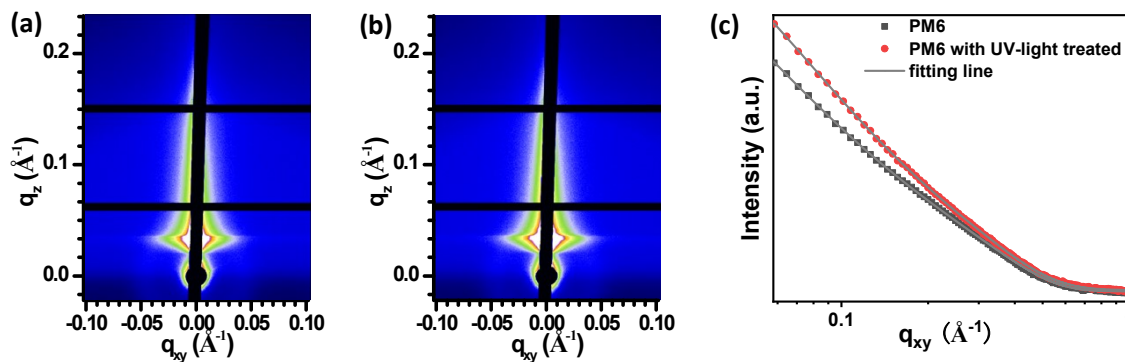


**Figure S2.** 2D GISAXS patterns of PM6 a) with or b) without UV-light treatment and c) 1D GISAXS profiles along out-of-plane.

**Table S1.** Fitting parameters of 1D GISAXS profiles for the pristine PM6 processed with or without UV-light treatment.

	$\phi_{PM6}$ (%)	$2R_{PM6}$ (nm)	$\xi_{PM6}$ (nm)	$D_{PM6}$	$R_{g-PM6}$ (nm)
as cast	18.0	12.6	30.9	2.0	53.5

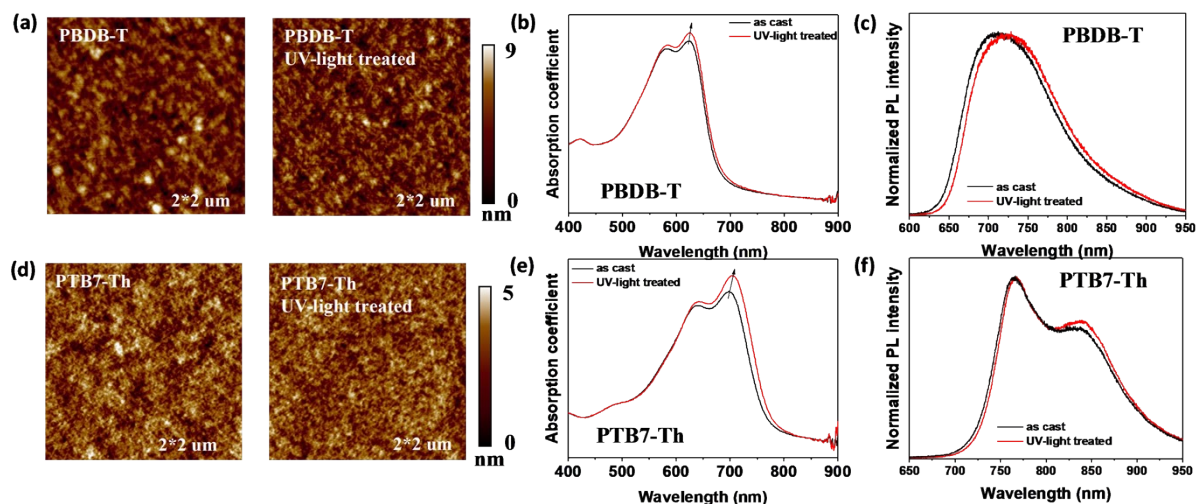


**Figure S3.** AFM height images of a) PBDB-T and d) PTB7-Th films; UV-vis spectra of b) PBDB-T and e) PTB7-Th films; PL spectra of c) PBDB-T and f) PTB7-Th films with or without UV-light treatment.

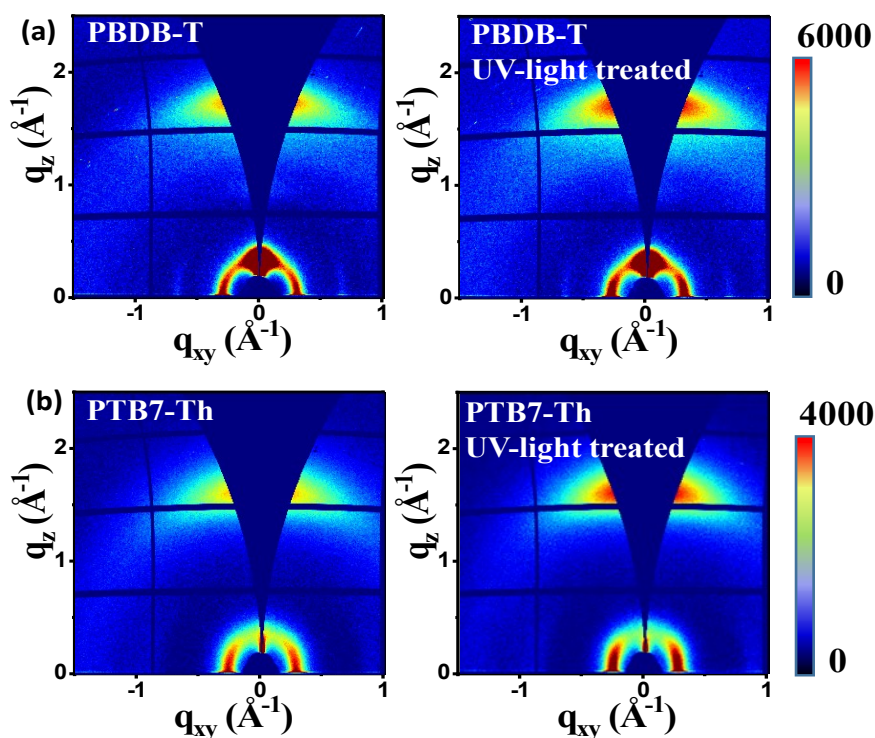


**Figure S4.** 2D GIWAXS patterns of a) PBDB-T and b) PTB7-Th films processed with or without UV-light treatment.

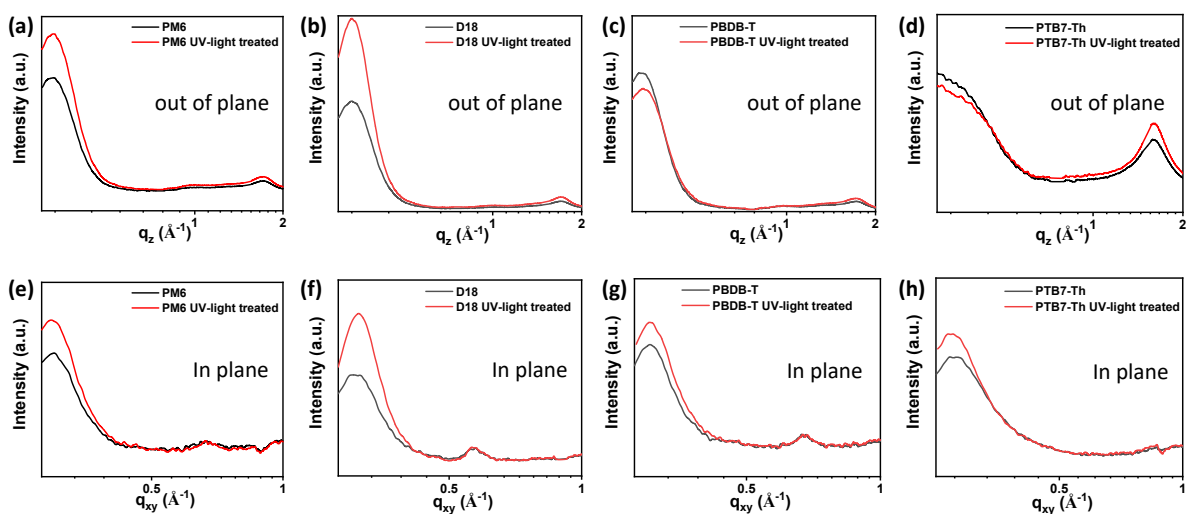


**Figure S5.** 1D GIWAXS profile of a) PM6, b) D18, c) PBDB-T and d) PTB7-Th films along out-of-plane; 1D GIWAXS profile of e) PM6, f) D18, g) PBDB-T and h) PTB7-Th films along in-plane.

**Table S2.** Detailed GIWAXS data of PM6, D18, PBDB-T and PTB7-Th films with or without UV-light treatment.

Films	Condition	(100)		(010)		CCL <sup>a)</sup> [Å]
		$q_z$ [Å <sup>-1</sup> ]	$d$ [Å]	$q_z$ [Å <sup>-1</sup> ]	$d$ [Å]	
<b>PM6</b>	as cast	0.30	20.94	1.71	3.67	20.20
<b>PM6</b>	UV-light treated	0.30	20.94	1.71	3.67	21.75
<b>D18</b>	as cast	0.31	20.27	1.70	3.70	21.75
<b>D18</b>	UV-light treated	0.31	20.27	1.70	3.70	23.56
<b>PBDB-T</b>	as cast	0.30	20.94	1.72	3.65	21.75
<b>PBDB-T</b>	UV-light treated	0.30	20.94	1.72	3.65	22.62
<b>PTB7-Th</b>	as cast	0.28	22.44	1.60	3.93	16.63
<b>PTB7-Th</b>	UV-light treated	0.28	22.44	1.60	3.93	17.14

a) Calculated from the Scherrer equation:  $CCL = 2\pi K / FWHM$ , where FWHM is the full-width at half-maximum of the peak and K is a shape factor (here we use 0.9).

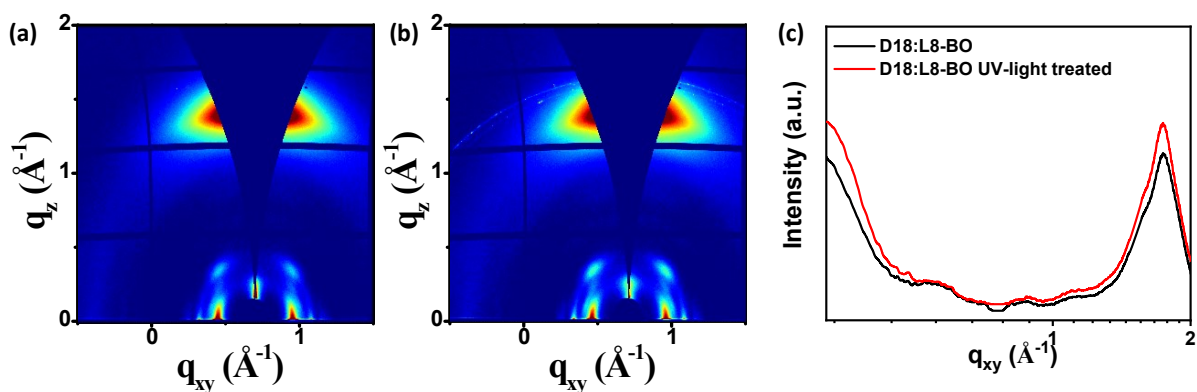


**Figure S6.** 2D GIWAXS patterns of D18:L8-BO films a) with or b) without UV-light treatment and c) 1D GIWAXS profile along out-of-plane.

**Table S3.** Photovoltaic metrics of OSCs with different UV-light treatment time.

OSCs	Condition	PCE <sub>max</sub> (PCE)	FF (%)	J <sub>SC</sub> (mA·cm <sup>-2</sup> )	V <sub>OC</sub> (V)
PM6:L8-BO	as cast	18.8 (18.5±0.3)	79.0	-27.0	0.89
PM6:L8-BO	UV-light treatment for 2 min	19.2 (18.9±0.2)	79.5	-27.2	0.89
PM6:L8-BO	UV-light treatment for 4 min	19.7 (19.4±0.2)	80.1	-27.5	0.89
PM6:L8-BO	UV-light treatment for 8 min	19.3 (18.8±0.4)	79.3	-27.6	0.88
OSCs	Condition	PCE <sub>max</sub> (PCE)	FF (%)	J <sub>SC</sub> (mA·cm <sup>-2</sup> )	V <sub>OC</sub> (V)
D18:L8-BO	as cast	18.9 (18.7±0.2)	78.3	-26.6	0.91
D18:L8-BO	UV-light treatment for 2 min	19.4 (19.0±0.3)	79.3	-26.9	0.91
D18:L8-BO	UV-light treatment for 4 min	19.6 (19.4±0.2)	79.8	-27.2	0.91
D18:L8-BO	UV-light treatment for 8 min	19.2 (18.9±0.3)	78.5	-27.2	0.90

OSCs	Condition	PCE <sub>max</sub> (PCE)	FF (%)	J <sub>SC</sub> (mA·cm <sup>-2</sup> )	V <sub>OC</sub> (V)
PBDB-T:L8-BO	as cast	13.4 (13.2±0.2)	68.5	-25.9	0.75
PBDB-T:L8-BO	UV-light treatment for 2 min	13.6 (13.3±0.3)	69.3	-26.1	0.75
PBDB-T:L8-BO	UV-light treatment for 4 min	13.9 (13.7±0.2)	70.3	-26.3	0.75
PBDB-T:L8-BO	UV-light treatment for 8 min	13.5 (13.2±0.3)	68.8	-26.5	0.74

OSCs	Condition	PCE <sub>max</sub> (PCE)	FF (%)	J <sub>SC</sub> (mA·cm <sup>-2</sup> )	V <sub>OC</sub> (V)
PTB7-Th:L8-BO	as cast	10.1 (10.0±0.1)	60.2	-23.4	0.72
PTB7-Th:L8-BO	UV-light treatment for 2 min	10.3 (10.1±0.2)	61.3	-23.3	0.72
PTB7-Th:L8-BO	UV-light treatment for 4 min	10.5 (10.3±0.1)	62.4	-23.4	0.72
PTB7-Th:L8-BO	UV-light treatment for 8 min	10.2 (10.2±0.1)	60.8	-23.6	0.71

**Table S4.** Photovoltaic metrics of OSCs with different photoactive layers.

OSCs	Condition	PCE <sub>max</sub> (PCE)	FF (%)	J <sub>SC</sub> (mA·cm <sup>-2</sup> )	J <sub>Cal</sub> (mA·cm <sup>-2</sup> )	V <sub>OC</sub> (V)
PBDB-T:L8-BO	as cast	13.4 (13.2±0.2)	68.5	-25.9	-25.2	0.75
PBDB-T:L8-BO	UV-light treated	13.9 (13.7±0.2)	70.3	-26.3	-25.5	0.75
PTB7-Th:L8-BO	as cast	10.1 (10.0±0.1)	60.2	-23.4	-22.7	0.72
PTB7-Th:L8-BO	UV-light treated	10.5 (10.3±0.1)	62.4	-23.4	-22.8	0.72



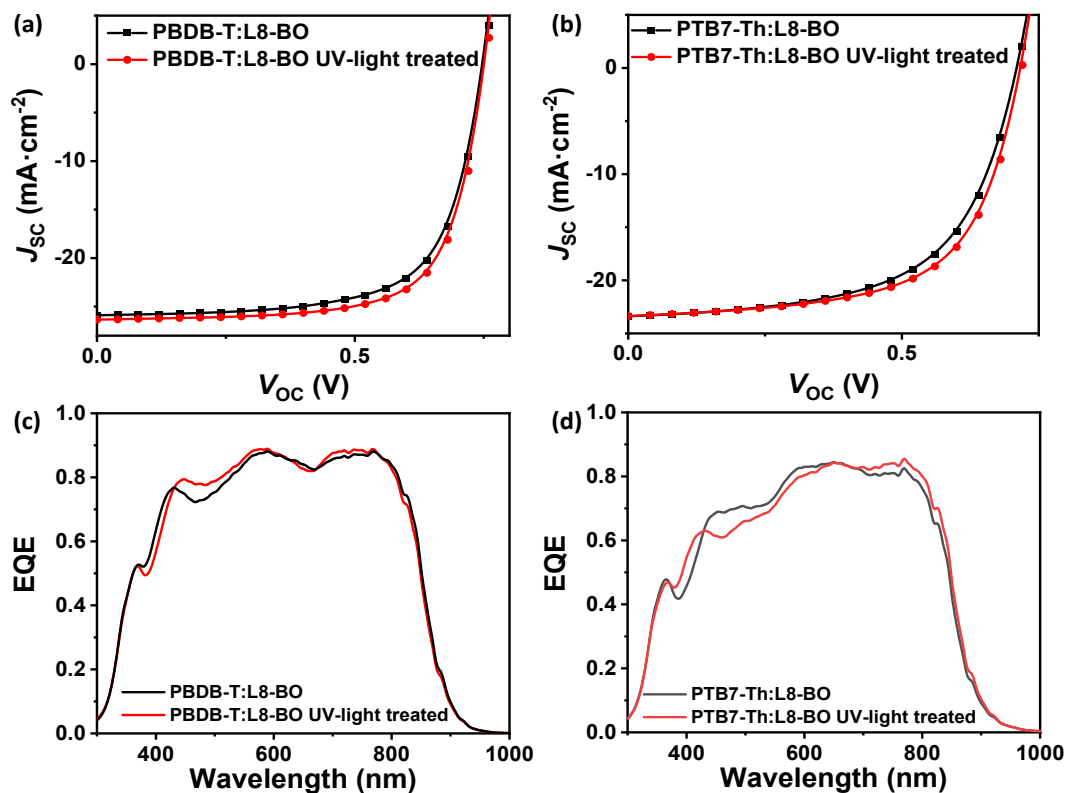


**Figure S7.**  $J$ - $V$  characteristics of (a) PBDB-T:L8-BO (b) PBDB-T: L8-BO based OSCs; EQE spectra of (c) PTB7-Th:L8-BO (d) PTB7-Th: L8-BO OSCs.

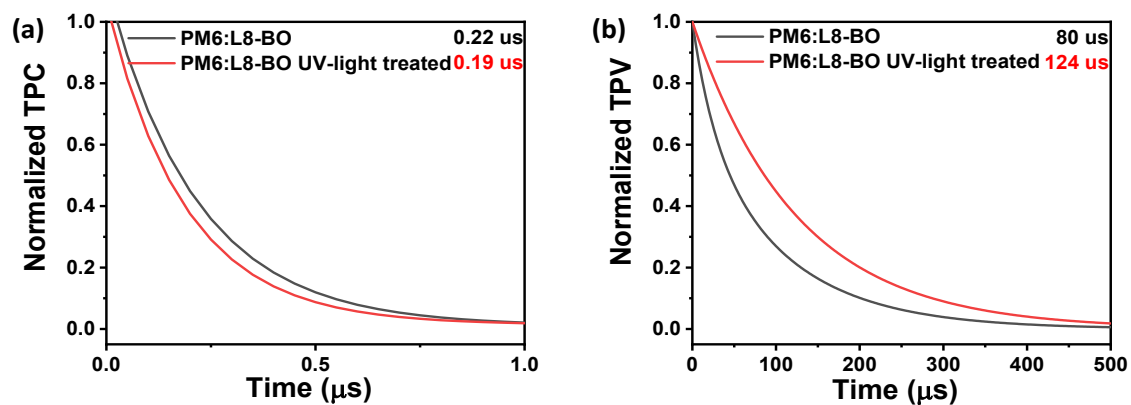


**Figure S8.** Normalized a) TPC and b) TPV of PM6:L8-BO with or without UV-light treatment.

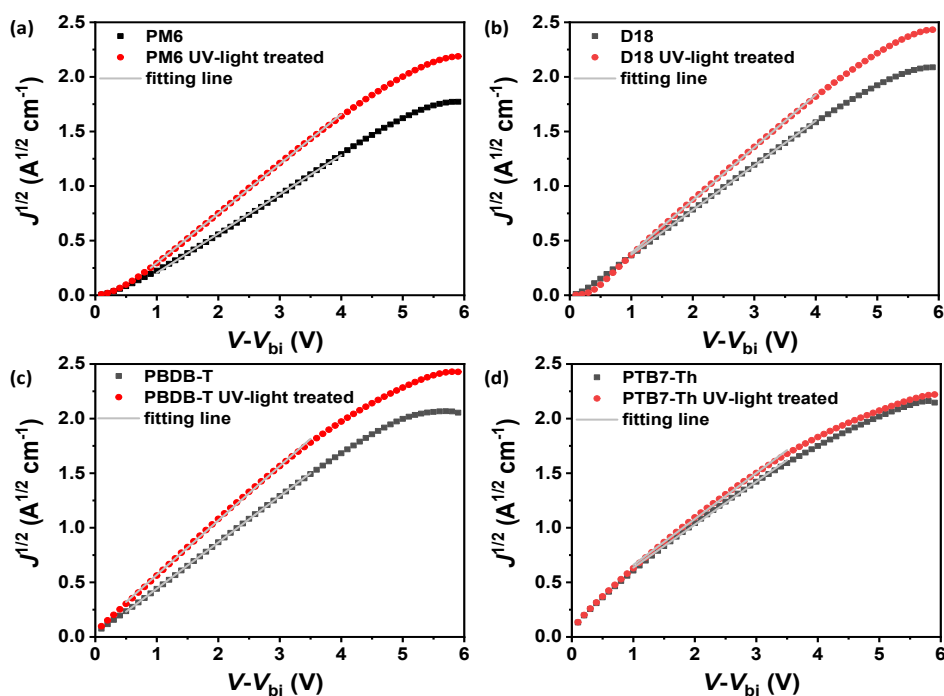


**Figure S9.**  $J^{1/2}$  vs  $V-V_{bi}$  plots of PM6, D18, PBDB-T and PTB7-Th with or without UV-light treatment.

**Table S4.** Hole mobilities of PM6, D18, PBDB-T and PTB7-Th with or without UV-light treatment.

polymer	condition	Hole mobilities ( $\mu_h$ ) ( $\text{cm}^2 \text{V}^{-1} \text{s}^{-1}$ )
PM6	as cast	$4.3 \times 10^{-4}$
PM6	UV-light treated	$6.9 \times 10^{-4}$
D18	as cast	$5.6 \times 10^{-4}$
D18	UV-light treated	$7.8 \times 10^{-4}$
PBDB-T	as cast	$3.1 \times 10^{-4}$
PBDB-T	UV-light treated	$4.3 \times 10^{-4}$
PTB7-Th	as cast	$2.7 \times 10^{-4}$
PTB7-Th	UV-light treated	$3.0 \times 10^{-4}$

## Reference

- 1 · C. Guo, Y. Fu, D. Li, L. Wang, B. Zhou, C. Chen, J. Zhou, Y. Sun, Z. Gan, D. Liu, W. Li and T. Wang, *Adv. Mater.*, 2023, **35**, e2304921.
- 2 · X. Xia, T.-K. Lau, X. Guo, Y. Li, M. Qin, K. Liu, Z. Chen, X. Zhan, Y. Xiao, P. F. Chan, H. Liu, L. Xu, G. Cai, N. Li, H. Zhu, G. Li, Y. Zhu, T. Zhu, X. Zhan, X.-L. Wang and X. Lu, *Nat. Commun.*, 2021, **12**, 6226.